Gas-Phase Thermochemistry of Polyhalide Anions

Katrina Emilia Nizzi, Cynthia Ann Pommerening, and Lee S. Sunderlin*

Department of Chemistry, Northern Illinois University, DeKalb, Illinois 60115

Received: June 2, 1998; In Final Form: July 14, 1998

A flowing afterglow−tandem mass spectrometer has been used to determine 0 K bond strengths in three hypervalent polyhalide ions: $D(Cl_2-Cl^-) = 99 \pm 5$ kJ/mol, $D(Br_2-Br^-) = 127 \pm 7$ kJ/mol, and $D(Br_2-Br_3^-) = 40 \pm 7$ kJ/mol. These bond strengths are close to the previously measured values $D(I_2-I^-) = 126 \pm 6$ kJ/mol and $D(I_2-I_3^-) = 49 \pm 6$ kJ/mol. In contrast, Cl_5^- and F_3^- are not formed at room temperature in the flowing afterglow. Solvation energies for the trihalides derived from this work and literature thermochemistry are inversely correlated with the size of the ion, in reasonable agreement with the predictions of the Born model. The electron affinities $EA(Cl_3) = 4.60 \pm 0.09$ eV and $EA(Br_3) = 4.55 \pm 0.10$ eV can also be derived. The gas-phase bond strengths are more consistent with the three center-four electron bond model than with the expanded octet model.

Introduction

Polyhalide anions are prototypical examples of hypervalent bonding.[1] For example, the central atom in X_3^- (X = I, Br, Cl, or F) has 10 valence electrons. Two models have been used to explain hypervalent bonding.[2] One involves "expansion of the octet" through use of low-lying d orbitals. Such expansion should become more prevalent lower in the periodic table because the energy gap between the valence p orbitals and the lowest empty d orbitals decreases. The expanded octet model has been largely discredited by recent theoretical work, which shows that d functions in the basis set primarily improve electron correlation or polarization.[3,4] It is still popular in general chemistry textbooks.[5]

The other model, due to Pimentel[6] and Hach and Rundle,[7] involves the three pσ orbitals on the linear X_3^- molecules, as shown in Scheme 1. These can be combined to form a strongly bonding orbital, a largely nonbonding orbital, and an antibonding orbital. Four electrons fill the lowest two orbitals, giving a three center-four electron bond. In contrast to the expanded octet, this type of bonding should not be strongly dependent on which halide is chosen.

The experimental trihalide bond strengths in aqueous solution are listed in Table 1. The data appear to be most consistent with the expanded octet model of hypervalent bonding. The nonobservation of F_3^- in solution[8] and the negative bond enthalpy for Cl_3^- suggest that accessible d orbitals are indeed necessary. However, X_3^- is much larger than X^-, and the charge is spread out over the whole molecule. Since X_3^- is more poorly solvated than $[X_2 + X^-]$, the bond strengths for solvated ions may reflect solvation effects more than the intrinsic bond strengths. The solvent effect can be substantial: $D(I_2-I^-) = 17$ kJ/mol in aqueous solution, ≈47 kJ/mol in acetone,[9] and 126 kJ/mol in the gas phase.[10] Therefore, gas-phase bond strengths are a better test of the nature of hypervalent bonding than solution-phase values. While the solution-phase bond strengths for many polyhalides were measured as long ago as the 19th century, experimental work on the gas-phase bond strengths has been remarkably sparse.[10−12]

* To whom correspondence should be addressed. Phone 815-753-6870, Fax 815-753-4802, e-mail sunder@niu.edu.

SCHEME 1

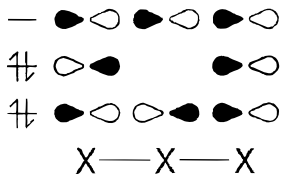

The bare polyhalide ions have been used as a test case for computational chemistry techniques. This work is summarized in Table 2. These results suggest that there is no dramatic trend in the X_2-X^- bond strength as X changes from I to F. However, these calculations are not consistent with each other. While the polyhalides might seem to be a simple computational subject, substantial difficulties are caused by large electron correlation effects, relativistic effects for the heavier nuclei, and the need for diffuse functions to properly model anions.[13−16] Accurate experimental results would be a useful benchmark for determining the computational method most appropriate to hypervalent systems. This determination is relevant to other systems that have similar electronic structures, such as S_N2 intermediates.[17]

Polyhalide ions, particularly polyiodides, are also of practical significance. Formation of the dark iodine−starch complex upon addition of iodine/iodide is still used as a test for the presence of starch; this complex involves the I_5^- anion.[18] Mixed polyhalide anions also have significance as analytical tools for the detection of halide ions because of their characteristic UV−vis spectra.[19] Such species have also been used as dopants to modify the electronic properties of polymers[20] and superconductors.[21] Hypervalent halogen compounds are useful reagents in organic synthesis.[22]

Experimental Section

The polyhalide bond strengths were measured using energy-resolved collision-induced dissociation in a flowing afterglow−tandem mass spectrometer (MS) described in detail previously.[10] The instrument consists of an ion source region, a flow tube, and the tandem mass spectrometer. The ion source used in these experiments is a dc discharge that is typically set at 1200 V

S1089-5639(98)02450-5 CCC: $15.00
Published on Web 09/09/1998

TABLE 1: Solvation Thermochemistry[a]

X	*D*-(X_2−$X^-_{(aq)}$)	radius-(X^-)[e]	radius-(X_3^-)[e]	ΔH_{sol}-(X^-)[e]	ΔH_{sol}-(X_2)[f]	ΔH_{sol}-(X_3^-)[g]
F		1.33		510		
Cl	2[b]	1.81	2.55	365	23	291
Br	6[c]	1.96	2.70	335	33	247
I	17[d]	2.2	2.85	290	41	222

[a] Energies in kJ/mol, radii in Å. All values at 298 K. [b] From $\Delta G = -4.1$ kJ/mol and $\Delta S = 19.5$ J/(mol K) for reaction 3 in aqueous solution (Hine, F.; Inuta, S. *Bull. Chem. Soc. Jpn.* **1968**, *41*, 71−75). The entropy is corrected from gas-phase chlorine to aqueous chlorine using the entropy of solution of $Cl_2 = -101.8$ J/(mol K) (ref *f*). [c] Ramette, R. W.; Palmer, D. A. *J. Solution Chem.* **1986**, *15*, 387−395. [d] Palmer, D. A.; Ramette, R. W.; Mesmer, R. E. *J. Solution Chem.* **1984**, *13*, 673−683. [e] Reference 30. [f] Woods, T. L.; Garrels, R. M. *Thermodynamic Values at Low Temperatures for Natural Inorganic Materials*; Oxford University Press: Oxford, 1987. [g] This work.

TABLE 2: Computational Bond Energies (kJ/mol at 0 K)

ref	I^-−I_2	Br^-−Br_2	Cl^-−Cl_2	F^-−F_2	method[a]
b	157	166	164	202	NLDF
c	118	159	166	198	NLDF
d	118	108	81	99	PHF
e	150	164	163		HF
f	114				PHF
f	135				NLDF
g	126				PHF
h	104				HF
i			98		PHF
j			136		HF
k				209	NLDF
l				110	NLDF
m				115	PHF
n				46	PHF

[a] NLDF is nonlocal density functional techniques, HF is Hartree−Fock, PHF is post-Hartree−Fock. See individual references for detailed descriptions of the computational techniques. [b] Landrum, G. A.; Goldberg, N.; Hoffmann, R. *J. Chem. Soc., Dalton Trans.* **1997**, 3605−3613. [c] Gutsev, G. L. *Russ. J. Phys. Chem.* **1992**, *66*, 1596−1599. [d] Reference 16. [e] Tasker, P. W. *Mol. Phys.* **1977**, *33*, 511−518. [f] Reference 15. [g] Reference 14. [h] Saethre, L. J.; Gropen, O.; Sletten, J. *Acta Chem. Scand. A* **1988**, *42*, 16−26. [i] Reference 12. [j] Riedel, E. F.; Willett, R. D. *Theor. Chim. Acta* **1976**, *42*, 237−246. [k] Sosa, C.; Lee, C.; Fitzgerald, G.; Eades, R. A. *Chem. Phys. Lett.* **1993**, *211*, 265−271. [l] Reference 13. [m] Ewig, C. S.; Van Wazer, J. R. *J. Am. Chem. Soc.* **1990**, *112*, 109−114. [n] Reference 3.

with 1 mA of emission current. The flow tube is a 92 cm × 7.3 cm i.d. stainless steel pipe, which operates at a buffer gas pressure of 0.4 Torr and flow rate of 200 standard cm^3/s. The buffer gas is He with up to 5% Ar added to stabilize the dc discharge source. Approximately 10^5 collisions with the buffer gas (and neutral halogen molecules) cool the ions to room temperature. The cooling should be efficient[23] because the polyhalide anions have low-frequency vibrational modes, which are given below.

The tandem MS is contained in a stainless steel box that is divided by interior partitions into five chambers. Differential pumping on the five chambers ensures that further collisions of the ions with the buffer gas after extraction from the flow tube are unlikely. The tandem MS includes a quadrupole mass filter, an octopole ion guide,[24] a second quadrupole mass filter, and a detector.

In the collision-induced dissociation (CID) experiments, ions are gently extracted from the flow tube through a 0.5 mm orifice by applying a 0−2 V potential to the nose cone at the end of the flow tube. The ions are then focused through electrostatic lenses into the first quadrupole mass filter (Q1). The reactant ions from Q1 are then focused into the octopole, which passes through a cell that contains the collision gas (Ar for Cl_3^- and Xe for Br_3^- and Br_5^-). From the octopole, the dissociated and unreacted ions are focused into a second quadrupole for mass analysis. The detector is an electron multiplier operating in pulse-counting mode.

The threshold energy for CID of a reactant ion is determined by modeling the intensity of product ions as a function of the reactant ion kinetic energy in the center-of-mass (CM) frame, E_{CM}. The reactant ion beam energy zero is measured using the octopole as a retarding field analyzer.[24,25] The first derivative of the beam intensity as a function of ion energy is approximately Gaussian, with a typical full width at half-maximum of 1.0 eV (1 eV = 96.49 kJ/mol). The laboratory energy E_{lab} in electronvolts is given by the octopole rod offset voltage measured with respect to the center of the Gaussian fit. This energy is corrected at low offset energies to account for truncation of the ion beam.[25]

Conversion to the CM frame is accomplished by use of $E_{CM} = E_{lab}m/(m + M)$, where m and M are the masses of the neutral and ionic reactants, respectively. To improve the signal, the mass filters were generally operated at low resolution, where all of the isotopic peaks were transmitted. For data collected in this manner, the average of the isotopic masses was used as the ion mass. For Cl_3^- and Br_3^-, some data sets were collected at higher resolution on an individual isotopic peak. The results were indistinguishable from the low mass resolution results. Similarly, the average xenon mass was used.

Total cross sections for reaction, σ_{total}, are calculated using eq 1,[25] where I is the intensity of the reactant ion beam, I_0 is

$$I = I_0 \exp(-\sigma_{total} n l) \tag{1}$$

the intensity of the incoming ion beam ($I_0 = I + \sum I_i$), and I_i are the intensities for each product ion. The number density of the neutral collision gas is n, and l is the effective collision cell length, 13 ± 2 cm.[10] Individual product cross sections σ_i are equal to $\sigma_{total}(I_i/\sum I_i)$.

To derive CID threshold energies, the threshold region of the data is fitted to the model function given in eq 2, where

$$\sigma(E) = \sigma_0 \sum_i g_i (E + E_i - E_T)^n / E \tag{2}$$

$\sigma(E)$ is the cross section for formation of the product ion at center-of-mass energy E, E_T is the desired threshold energy, σ_0 is a scaling factor, n is an adjustable parameter, and i denotes rovibrational states having energy E_i and population g_i ($\sum g_i = 1$). The CRUNCH program written by Prof. P. B. Armentrout and co-workers is used in the threshold analysis described above. Broadening due to the thermal motion of the collision gas (Doppler broadening) and the kinetic energy distribution of the reactant ion are accounted for by the program.

Experimental stretching frequencies for the trihalides[3] and calculated bending frequencies for F_3^- [3] and Br_3^- [26] are used in the above data analysis. The bending frequency for Cl_3^- is estimated by interpolating the force constants for F_3^- and Br_3^-. Rotational constants for these molecules are derived from calculated bond lengths.[16] Frequencies for Br_5^- are estimated using the force constants and geometries computed for I_5^-.[15] The rotational and vibrational frequencies used are summarized in Table 3. The internal energy is small (6−10 kJ/mol for the triatomic molecules and 21 kJ/mol for Br_5^-) and only moderately sensitive to the vibrational frequencies. The effect of incomplete dissociation on the experimental time scale (kinetic shifts) is negligible for the triatomic atoms and 0−1 kJ/mol for

TABLE 3: Spectroscopic Constants[a]

species	rotation	vibration
F_3^-	146 (×2)	277 (×2), 461, 550
Cl_3^-	43 (×2)	156 (×2), 242, 268
Br_3^-	15 (×2)	81 (×2), 168, 187
Br_5^-	3.1, 3.6, 24	18, 67, 71, 72, 76, 112, 142, 181, 199

[a] Vibrational constants in cm^{-1}, rotational constants in 10^{-3} cm^{-1}. See text for sources.

Br_5^-, depending on whether the transition state for dissociation is loose (product-like) or tight (reactant-like). Therefore, the derived thresholds are only slightly sensitive to the spectroscopic parameters. Because the reactant and product internal energies are taken into account, the reaction thresholds correspond to bond energies (or enthalpies) at 0 K.

The collision gas pressure can influence the observed cross sections because an ion that is not sufficiently energized by one collision with the target gas may gain enough energy in a second collision to be above the dissociation threshold. Such collisions can lead to a measured threshold that is too low. This is accounted for by linearly extrapolating data taken at several pressures to a zero pressure cross section,[27] which is then fit with the method described above.

Results

When small amounts of bromine are added to the ion source, Br^- and Br_3^- are the main species observed. A trace of Br_2^- is also seen. The Br^- is due to dissociative attachment of an electron to Br_2, while Br_2^- is due to collisionally stabilized electron attachment. At higher flow rates, the Br^- and Br_2^- are depleted, and Br_3^- and Br_5^- are the dominant ions. These are due to collisionally stabilized attachment of Br_2 to Br^- and Br_3^-.

Although several precursors for Cl_3^- were tested, the best results are obtained by simply introducing Cl_2 into the ion source. Use of CH_xCl_{4-x} ($x = 0-2$) as a Cl^- precursor leads to impurities near the mass range of Cl_3^-. Use of SO_2Cl_2 as a Cl_2 donor gives lower intensities of Cl_3^-.

No Cl_5^- is observed with Cl_2 partial pressures as high as 50 mTorr, implying that Cl_5^- is less stable than Br_5^-. Similarly, attempts to make F_3^- by addition of up to 6 mTorr of F_2 to the flow tube were also unsuccessful. The F^-/F_3^- ratio was at least 80:1, and the minimal signal at the mass of F_3^- may have been due to an impurity. This indicates that F_3^- is not as stable as the other three trihalides. If it is assumed that equilibrium has been reached under the conditions described above, $D(F^- - F_2) \leq 54$ kJ/mol can be derived using the data for F_3^- and F_2 in Table 3 and ref 28, respectively. However, collisional stabilization of the F_3^- may not be sufficiently rapid to ensure equilibrium.

The cross sections for CID of Cl_3^-, Br_3^-, and Br_5^- are shown in Figures 1−3. The reaction channels observed are given in reactions 3−7. For X_3^-, the two products correspond to

$$Cl_3^- \rightarrow Cl^- + Cl_2 \quad (3)$$

$$Cl_3^- \rightarrow Cl + Cl_2^- \quad (4)$$

$$Br_3^- \rightarrow Br^- + Br_2 \quad (5)$$

$$Br_3^- \rightarrow Br + Br_2^- \quad (6)$$

$$Br_5^- \rightarrow Br_3^- + Br_2 \quad (7)$$

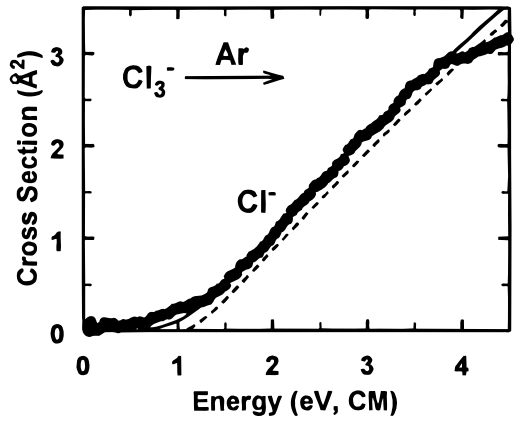

Figure 1. Appearance curve for collision-induced dissociation of Cl_3^- as a function of kinetic energy in the center-of-mass frame. The solid line is the model appearance curve calculated using eq 2 and convoluted as discussed in the text. The dashed line is the unconvoluted fit. The fitting parameters are given in Table 5.

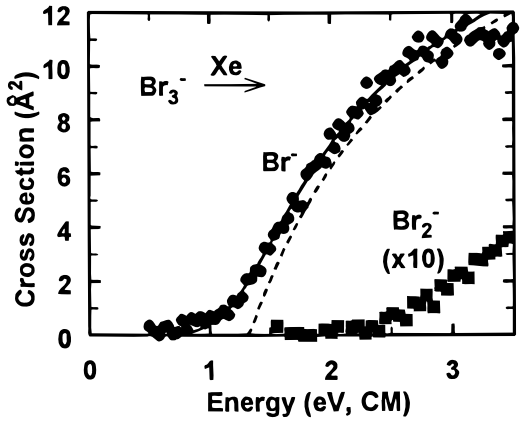

Figure 2. Appearance curves for collision-induced dissociation of Br_3^- as a function of kinetic energy in the center-of-mass frame. The solid line is the model appearance curve calculated using eq 2 and convoluted as discussed in the text. The dashed line is the unconvoluted fit. The fitting parameters are given in Table 5.

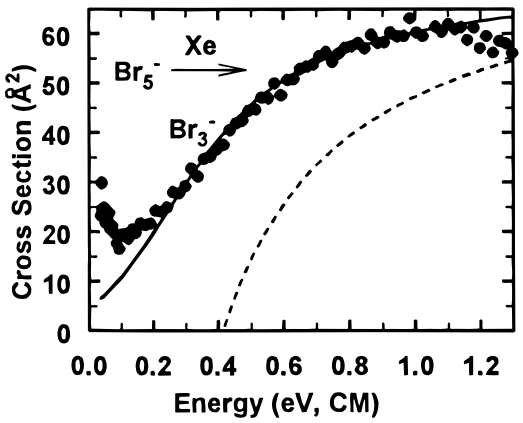

Figure 3. Appearance curve for collision-induced dissociation of Br_5^- as a function of kinetic energy in the center-of-mass frame. The solid line is the model appearance curve calculated using eq 2 and convoluted as discussed in the text. The dashed line is the unconvoluted fit. The fitting parameters are given in Table 5.

cleavage of an X_2-X bond with a competition between X_2 and X for possession of the extra electron. As seen in Table 4, it is always lower in energy for X to retain the electron. The difference in energy goes from 1.22 eV for X = Cl to 0.82 eV for X = Br to 0.54 eV for X = I. The X^-/X_2^- cross section ratio at a collision energy of 4 eV is 50 for X = Cl, 20 for X

TABLE 4: Gas-Phase Thermochemistry[a]

X	EA(X)[b]	EA(X_2)[b]	EA(X_3)	D(X−X)[b]	D(X_2−X)	D(X_2−X^-)	D(X_2−X_3^-)
F	3.401	3.01 ± 0.07		155			
Cl	3.613	2.4 ± 0.20	4.60 ± 0.09[c]	239	4 ± 7[e]	99 ± 5[c]	
Br	3.364	2.55 ± 0.10	4.55 ± 0.10[c]	170	13 ± 7[e]	127 ± 7[c]	40 ± 7[c]
I	3.059	2.52 ± 0.10	4.15 ± 0.12[d]	149	21 ±10[f]	126 ± 6[d]	49 ± 6[d]

[a] Electron affinities in eV; other thermochemical values in kJ/mol. All values at 0 K. [b] Reference 27. [c] This work. [d] Reference 10. [e] Kawasaki, M.; Sato, H.; Inoue, G. *J. Phys. Chem.* **1989**, *93*, 7571−7575. Error limits are estimated from the range of values given. [f] Kang, S. H.; Kunc, J. A. *Phys. Rev. A* **1991**, *44*, 3596−3605. See also ref 10.

TABLE 5: CID Threshold Measurements[a]

reaction	threshold	n
3	99 ± 5	1.7 ± 0.2
5	127 ± 7	1.5 ± 0.3
7	40 ± 7	0.8 ± 0.2

[a] Threshold values in kJ/mol. See text for discussion of the fitting parameter n.

= Br, and 10 for X = I. This is consistent with the decreasing energy gap between the two channels.

The data for CID of Br_5^- show a nonzero cross section even at the lowest translational energies. This is attributed to ions with enough internal energy to be very near the dissociation threshold, which is only twice the average internal energy content of the molecules. These molecules should have a very high cross section for dissociation with even low-energy collisions. The data at translational energies below 25 kJ/mol are not included in the fit.

The eq 2 fitting parameters for the data are given in Table 5. The dissociation thresholds correspond to the bond energies at 0 K, which are reported in Table 4. Uncertainties in the reaction thresholds are derived from the standard deviation of the fits to individual data sets and the uncertainty in the energy scale (±0.1 eV lab). The parameters for loss of X_2 from the trihalides are remarkably similar: for I_3^-, n = 1.5 ± 0.2 and the threshold energy is 126 ± 6 kJ/mol.[10] The data for reactions 4 and 6 cannot be fit reliably because of the small size of the cross section and the slow rise from threshold due to competition from loss of X_2.

The 0 K bond energies can be converted into bond energies at 298 K using the spectroscopic constants. The results are D^{298}(Cl_2−Cl^-) = 97 ± 5 kJ/mol, D^{298}(Br_2−Br^-) = 125 ± 7 kJ/mol, and D^{298}(Br_2−Br_3^-) = 36 ± 7 kJ/mol. The bond enthalpies are higher by ΔPV (=RT): DH^{298}(Cl_2−Cl^-) = 99 ± 5 kJ/mol, DH^{298}(Br_2−Br^-) = 127 ± 7 kJ/mol, and DH^{298}(Br_2−Br_3^-) = 38 ± 7 kJ/mol. The bond enthalpies and the heats of formation of the fragments,[28] $\Delta_f H^{298}(Cl_{2(g)})$ = 0.0 kJ/mol, $\Delta_f H^{298}(Cl^-_{(g)})$ = −227.3 kJ/mol, $\Delta_f H^{298}(Br_{2(g)})$ = 30.9 kJ/mol, and $\Delta_f H^{298}(Br^-_{(g)})$ = −212.7 kJ/mol, can be combined to give $\Delta_f H^{298}(Cl_3^-_{(g)})$ = −326 ± 5 kJ/mol, $\Delta_f H^{298}(Br_3^-_{(g)})$ = −309 ± 7 kJ/mol, and $\Delta_f H^{298}(Br_5^-_{(g)})$ = −316 ± 10 kJ/mol.

Discussion

Solvation Energies. Measurements of association constants as a function of temperature have been used to derive the aqueous bond strengths in Table 1. The difference between the bond strengths in the gas phase and in solution equals the difference between the enthalpies of solvation of [X^- + X_2] and X_3^-. This thermochemistry is summarized in Table 1. The solvation energy decreases with increasing size of the anion. The standard Born Model for solvation energetics[29] states that the free energy of solvation should be proportional to $1/r_{anion}$. Figure 4 shows the free energies of solvation plotted against the ionic radii.[30] The linear regression to the data, shown in Figure 4, has a slope of 648 kJ Å/mol and an x-intercept of −19 kJ/mol; a fit to more data gives a slope of 686 kJ Å/mol.[29] The magnitude of this slope demonstrates the significance of solvent effects on bond strengths and indicates that even if F_3^- were as strongly bound as the other trihalides in the gas phase, it would not be stable in solution. More sophisticated models of solvation effects have been derived;[30] the precision of the data does not warrant a more detailed treatment.

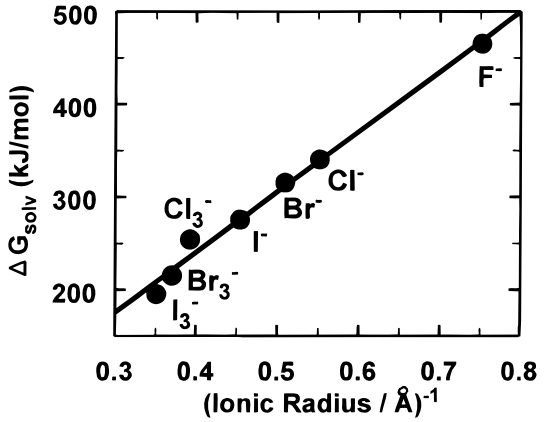

Figure 4. Aqueous solvation energy of halide and trihalide anions as a function of ionic radius. The line is a linear regression fit to the data.

The solvation energies of the trihalide anions are important for understanding the mechanism of halogen uptake by saltwater droplets. While dihalogen molecules are not very soluble in pure water, formation of trihalide anions in monohalide solutions increases the rate of removal of dihalogens from the gas phase.[12,31,32] This is a complex subject because the process fundamentally occurs at the gas−liquid interface rather than in the bulk solution.

Electron Affinities. From this work and previously known thermochemistry, it is possible to use eq 8 to derive the electron

$$EA(X_3) = EA(X) + D(X_2 - X^-) - D(X_2 - X) \quad (8)$$

affinity of X_3. The relevant data are again summarized in Table 4. Nearly all of the molecules with known higher electron affinities are metal halides, hydrogen-bonded species such as ClHCl, or perfluorinated hydrocarbons.[28] If the trihalides are thought of as halogen halides, then all of these systems fit a pattern of central moieties with multiple halide ligands.

Comparison to Previous Experiments. In a previous determination of the trichloride bond strength,[11] reactions 9−11 were observed and reactions 9 and 11 were believed to be in equilibrium in a high-pressure ion source at essentially room temperature. The enthalpy for reaction 9 was estimated to be 4 kJ/mol.[11] Since elimination of Cl_2 from SO_2Cl_2 is 58 kJ/mol endothermic,[28] this leads to D(Cl^-−Cl_2) = 54 kJ/mol. However, reactions 10 and 11 can be added together to give reaction 12. If reaction 12 is exothermic, as suggested by the observation of reactions 10 and 11, then D(Cl^-−Cl_2) ≥ 116 kJ/mol. The discrepancy between these two values for D(Cl^-−Cl_2) indicates

$$Cl^- + SO_2Cl_2 \rightleftarrows Cl_3^- + SO_2 \quad (9)$$

$$Cl^- + SO_2Cl_2 \rightarrow SO_2Cl^- + Cl_2 \quad (10)$$

$$SO_2Cl^- + SO_2Cl_2 \rightleftarrows Cl_3^- + 2SO_2 \quad (11)$$

$$Cl^- + 2SO_2Cl_2 \rightarrow Cl_2 + Cl_3^- + 2SO_2 \quad (12)$$

that equilibrium had not been established and that the thermochemistry from these experiments is unreliable. The 99 kJ/mol bond enthalpy derived in this work indicates that reaction 12 is endothermic by about 17 kJ/mol, which suggests that reactions 10 and 11 are both slightly endothermic.

Two groups have noted that Cl_2 will rapidly displace D_2O from $Cl^-(D_2O)$ under room-temperature conditions.[12,33] This implies that $D(Cl^- - Cl_2) \geq D(Cl^- - D_2O) = 62$ kJ/mol.[34] This is in agreement with the bond strength derived in this work.

Herschbach and co-workers[35] determined the electron affinity of Cl_3 by measuring the translational energy threshold for dissociative electron transfer from Rb to $(Cl_2)_2$. They derived $EA(Cl_3) = 4.6$ or 5.1 eV depending on the method of analysis. The first number is in excellent agreement with the present results.

Comparison to Theory. When the computational results in Table 2 are compared to the experimental values, several trends emerge. There is no strong correlation between the level of calculation and the agreement with experiment, but three recent calculations at very high levels of theory are in good agreement with the present results.[12,14,15] The density functional calculations give bond strengths that are consistently too high. The agreement is best for I_3^- and gets consistently worse for smaller ions, with most of the calculations for smaller ions overestimating the bond strength. Apparently, the errors from incomplete basis sets (which tend to give bond strengths that are too low) and inaccurate estimates of correlation energy (which tend to give bond strengths that are too high) often cancel.[13] The effective core potentials used for the heavier atoms do not appear to cause any inaccuracy. However, it is clear from the widely scattered results for F_3^-, and the general disagreement with the experimental evidence for a weak bond, that correlation effects are still not well understood for this anion.

Implications for Hypervalent Bonding. The most fundamental question this work addresses is the participation of d orbitals in hypervalent bonding. The first conclusion is that solution-phase bond strengths can give misleading periodic trends. The gas-phase bond strengths do not fit perfectly with either the expanded octet model or the simplest interpretation of the three center-four electron model, which suggests that all trihalide bonds should be about equal. To resolve this discrepancy, two other sets of data should be considered: the electron affinities of the halogen atoms X and the bond strengths of X_2. Neither of these sets of molecules is hypervalent, but both show very nonmonotonic periodic trends. In both cases, it is clear that placing more electrons around a fluorine atom is less favorable than placing them around a chlorine atom. This can be attributed to electron−electron repulsion in the very small fluorine systems. It is not surprising that F_3^- is weakly bound because F_2 and F^- are also weakly bound. Thus, the bond energies in this paper are consistent with the three center-four electron model when the unique nature of fluorine is considered.

Acknowledgment. We thank the American Society for Mass Spectrometry for partial support of this work through a research award to L.S.S. and the College of Liberal Arts and Sciences at NIU for an Undergraduate Research Apprenticeship awarded to K.N. Acknowledgment is also made to the donors of the Petroleum Research Fund, administered by the American Chemical Society, for the partial support of this research. We thank Peter Armentrout for the use of the CRUNCH program and Steven Bachrach for useful discussions.

References and Notes

(1) Tebbe, K.-F. Polyhalogen Cations and Polyhalide Anions. In *Homoatomic Rings, Chains and Macromolecules of Main Group Elements*; Rheingold, A. L., Ed.; Elsevier: Amsterdam, 1977.

(2) The historical background of this issue is discussed in: Reed, A. E.; Schleyer, P. v. R. *J. Am. Chem. Soc.* **1990**, *112*, 1434−1445.

(3) Cahill, P. A.; Dykstra, C. E.; Martin, J. C. *J. Am. Chem. Soc.* **1985**, *107*, 6359−6362.

(4) Magnusson, E. *J. Am. Chem. Soc.* **1990**, *112*, 7940−7951. Magnusson, E. *J. Am. Chem. Soc.* 1993, *115*, 1051−1061.

(5) See, for example: Chang, R. *Chemistry*, 6th ed.; McGraw-Hill: Boston, 1998. McMurry, J.; Fay, R. C. *Chemistry*; 2nd ed.; Prentice Hall: Upper Saddle River, NJ, 1998. Silverberg, M. *Chemistry*; Mosby: St. Louis, 1996.

(6) Pimentel, G. C. *J. Chem. Phys.* **1951**, *19*, 446−448.

(7) Hach, R. J.; Rundle, R. E. *J. Am. Chem. Soc.* **1951**, *73*, 4321−4324.

(8) The trifluoride anion has been observed in rare-gas matrixes: Ault, B. S.; Andrews, L. *J. Am. Chem. Soc.* **1976**, *98*, 1591−1593. Ault, B. S.; Andrews, L. *Inorg. Chem.* **1977**, *16*, 2024−2028. Hunt, R. D.; Thompson, C.; Hassanzadeh, P.; Andrews, L. *Inorg. Chem.* **1994**, *33*, 388−391.

(9) Nelson, I. V.; Iwamoto, R. T. *J. Electroanal. Chem.* **1964**, *7*, 218−221.

(10) Do, K.; Klein, T. P.; Pommerening, C. A.; Sunderlin, L. S. *J. Am. Soc. Mass Spectrom.* **1997**, *8*, 688−696.

(11) Robbiani, R.; Franklin, J. L. *J. Am. Chem. Soc.* **1979**, *101*, 3709−3715.

(12) Seeley, J. V.; Morris, R. A.; Viggiano, A. A. *J. Phys. Chem.* **1996**, *100*, 15821−15826.

(13) Heard, G. L.; Marsden, C. J.; Scuseria, G. E. *J. Phys. Chem.* **1992**, *96*, 4359−4366.

(14) Danovich, D.; Hrušák, J.; Shaik, S. *Chem. Phys. Lett.* **1995**, *233*, 249−256.

(15) Sharp, S. B.; Gellene, G. I. *J. Phys. Chem A* **1997**, *101*, 2192−2197.

(16) Novoa, J. J.; Mota, F.; Alvarez, S. *J. Phys. Chem.* **1988**, *92*, 6561−6566.

(17) Chabync, M. L.; Craig, S. L.; Regan, C. K.; Brauman, J. I. *Science* **1998**, *279*, 1882−1886.

(18) Teitelbaum, R. C.; Ruby, S. L.; Marks, T. J. *J. Am. Chem. Soc.* **1980**, *102*, 3322−3328.

(19) Wang, T. X.; Kelley, M. D.; Cooper, J. N.; Beckwith, R. C.; Margerum, D. W. *Inorg. Chem.* **1994**, *33*, 5872−5878.

(20) Harada, I.; Furukawa, Y.; Tasami, M.; Shirakawa, H.; Ikeda, S. *J. Chem. Phys.* **1980**, *76*, 4746−4757.

(21) Williams, J. M.; Wang, H. H.; Emge, T. J.; Geiser, U.; Beno, M. A.; Leung, P. C. W.; Carlson, K. D.; Thorn, R. J.; Schultz, A. J.; Whangbo, M.-H. *Prog. Inorg. Chem.* **1987**, *35*, 51−218.

(22) Varvoglis, A. *Hypervalent Iodine in Organic Synthesis*; Academic: San Diego, 1997. Stang, P. J.; Zhdankin, V. V. *Chem. Rev.* **1996**, *96*, 1123−1178. Schlama, T.; Gabriel, K.; Gouverneur, V.; Mioskowski, C. *Angew. Chem., Int. Ed. Engl.* **1997**, *36*, 2342−2344. Zhdankin, V. V. *Rev. Heteroatom Chem.* **1997**, *17*, 133−151.

(23) Smith, D.; Adams, N. G. *Adv. At. Mol. Phys.* **1988** *24*, 1−49 and references therein.

(24) Gerlich, D. *Adv. Chem. Phys.* **1992**, *82*, 1−176.

(25) Ervin, K. M.; Loh, S. K.; Aristov, N.; Armentrout, P. B. *J. Phys. Chem.* **1983**, *87*, 3593. Ervin, K. M.; Armentrout, P. B. *J. Chem. Phys.* **1985**, *83*, 166−189.

(26) Christe, K. O.; Dixon, D. A.; Minkwitz, R. *Z. Anorg. Allg. Chem.* **1992**, *612*, 51−55.

(27) Loh, S. K.; Lian, L.; Hales, D. A.; Armentrout, P. B. *J. Chem. Phys.* **1989**, *90*, 5466−5485. Schultz, R. H.; Crellin, K. C.; Armentrout, P. B. *J. Am. Chem. Soc.* **1991**, *113*, 8590−8601.

(28) Mallard, W. G., Linstrom, P. J., Eds. *NIST Chemistry WebBook*, NIST Standard Reference Database Number 69, March 1998, National Institute of Standards and Technology, Gaithersburg, MD, 20899 (http://webbook.nist.gov).

(29) Atkins, P. *Physical Chemistry*, 6th ed.; Freeman: New York, 1998; Chapter 10.

(30) Marcus, Y. *Biophys. Chem.* **1994**, *51*, 111−127. The ionic radius and solvation entropy for Cl_3^- are linearly extrapolated from values for I_3^- and Br_3^- in this work.

(31) Hu, J. H.; Shi, Q.; Davidovits, P.; Worsnop, D. R.; Zahniser, M. S.; Kolb, C. E. *J. Phys. Chem.* **1995**, *99*, 8768−8776. Davidovits, P.; Hu, J. H.; Worsnop, D. R.; Zahniser, M. S.; Kolb, C. E. *Faraday Discuss.* **1995**, *100*, 65−81.

(32) Coe, J. V. *J. Phys. Chem. A* **1997**, *101*, 2055−2063.

(33) Wincel, H.; Mereand, E.; Castleman, A. W., Jr. *J. Phys. Chem.* **1995**, *99*, 15678−15685.

(34) Keesee, R. G.; Castleman, A. W., Jr. *J. Phys. Chem. Ref. Data* **1986**, *15*, 1011−1071. Entropy effects neglected in bond strength.

(35) Bowen, K. H.; Liesegang, G. W.; Sanders, R. A.; Herschbach, D. R. *J. Phys. Chem.* **1983**, *87*, 557−565.